

Evolution of Electrooptical Properties of Epoxy–Amine Thermoset/Liquid Crystal Blends During Polymerization After the Gel Point of the Polymer Matrix

Lucas Sannier,¹ Humaira Masood Siddiqi,^{2,*} Ulrich Maschke,¹ Michel Dumon²

¹Laboratoire de Chimie Macromoléculaire, UPRESA CNRS 8009, Université des Sciences et Techniques de Lille, bâtiment C6, F-59 655 Villeneuve d'Ascq Cedex, France

²Laboratoire des Matériaux Macromoléculaires, UMR CNRS 5627, Institut National des Sciences Appliquées de Lyon–INSA Lyon, bâtiment Jules Verne, 20 avenue Albert Einstein, F-69 621 Villeurbanne Cedex, France

Received 27 July 2003; accepted 31 December 2003

ABSTRACT: Polymer dispersed liquid crystals (PDLC) were obtained by polymerization-induced phase separation of the nematic E7 liquid crystal in a reactive diepoxide–diamine thermosetting matrix prepared by polycondensation (in two thermal steps). The evolution of some important electrooptical characteristics (transmittance in the off-state, threshold voltage, maximum transmittance of the on-state, transmittance at maximum applied voltage) were studied at three different reaction conversions of the polymer matrix beyond the gel point. The electrooptical curves greatly depended on the reaction conversion, especially beyond the gel point of the polymer matrix. It was found that the transmission in both the off-state and the on-state decreased with the extent of cure. In addition, threshold and saturation voltages increased with the reaction conversion. The elec-

trooptical curve showed unusual behavior at approximately 60% of reaction conversion (i.e., near the gel conversion). At higher conversions, the expected normal mode was recovered. We discussed these electrooptical characteristics in the light of the very significant evolution of some properties of the crosslinked polymer matrix (glass-transition temperatures, concentration of crosslink points, molar mass, and weight fraction of the residual uncrosslinked oligomers), whereas the droplet morphology did not exhibit dramatic changes. © 2004 Wiley Periodicals, Inc. *J Appl Polym Sci* 92: 2621–2628, 2004

Key words: gelation; polymer dispersed liquid crystals (PDLCs); crosslinking; thermosets; morphology

INTRODUCTION

Polymer blends based on a crosslinked matrix often result from a polymerization-induced phase separation process^{1,2}: first, monomer(s) or oligomer(s) are mixed with an additive to form a homogeneous solution (the additive is a low molar mass or a polymeric molecule, reactive or not reactive with the monomers); second, the monomers are polymerized and the additive separates mainly because of the decrease in the entropy of mixing of the system (i.e., because of the increase in molar mass). When the additive is a low molar mass liquid crystal (LC), depending on the weight fraction of LC and the morphology of the LC phase, the blends were designated as either polymer dispersed liquid crystals (PDLC), polymer network liquid crystals (PNLC), or polymer stabilized liquid crystals (PSLC).^{3–5} These materials are known to ex-

hibit an optical contrast change under an electric field and thus are used in electrooptical applications.⁶

For example, the optical switching of PDLCs between an opaque and transparent state in the visible range requires a microcomposite material with submicron or microsized dispersed LC droplets. Persistent problems, however, include the reproducibility and control of materials in terms of the *in situ* generated morphologies and understanding of the factors or events that influence these morphologies during the formation process of the microcomposites. It is generally admitted that the electrooptical properties of PDLC, for example, depend primarily on the type of morphology (size, size distribution, shape, orientation, and number density of LC droplets) but also depend on the interactions between the LC domains and the polymer matrix, both surface properties (interfacial interactions/strength of anchoring of LC molecules, existence of an interphase, etc.) and volume properties (composition and purity of the LC phase, configuration of the LC molecules, solubility of LC in the polymer matrix or swelling of the network if the polymer matrix is crosslinked). In the latter case (crosslinked matrices), the elastic properties may also influence the optical response. During the polymeriza-

*Permanent address: Department of Chemistry, Quad-i-Azam University, 46 002 Islamabad, Pakistan.

Correspondence to: M. Dumon (lmm@insa-lyon.fr)

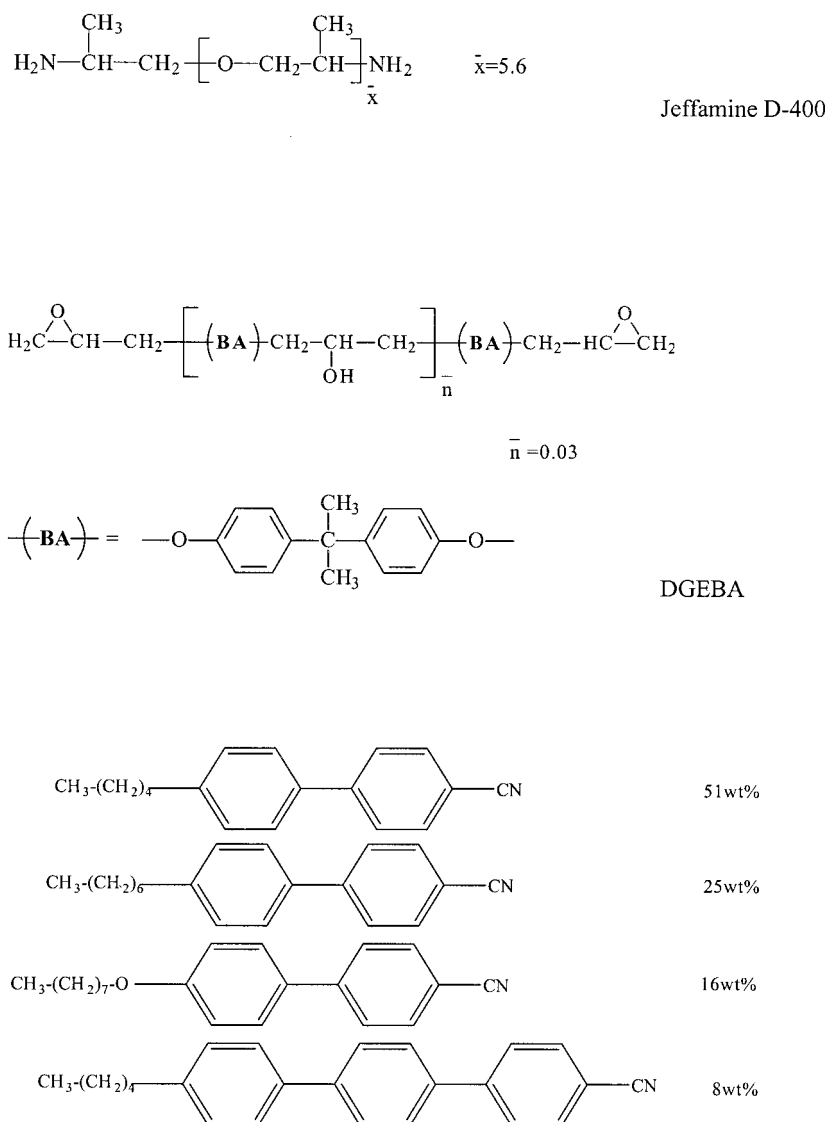


Figure 1 Chemical structures of the diepoxy DGEBA, diamine jeffamine D-400 monomers (matrix precursors), and liquid crystal E7 BL001.

tion process, elastic properties of the polymer matrix appear beyond a reaction conversion called gel point or gel conversion.⁷ Gelation is usually considered to be favorable, in that it fixes the morphology of LC droplets even if, in some cases, some morphologies are able to change after the gel point.²

In this article, we present the evolution of a PDLC material, at three different reaction conversions of the polymer matrix near or beyond the gel point, in a diepoxide–diamine reactive thermosetting polymer/LC composite. We point out factors (glass-transition temperatures, concentration of crosslink points, molar mass and weight fraction of the residual uncrosslinked oligomers) that heavily influence the evolution of the electrooptical behavior in the course of the reaction. The electrooptical characteristics under consideration are transmittance in the off-state, thresh-

old voltage, maximum transmittance of the on-state, and transmittance at maximum applied voltage.

EXPERIMENTAL

Materials and sample preparation

Diglycidyl ether of bisphenol A (DGEBA) resin (DER 332, with an average degree of polymerization $n = 0.03$; Dow Chemicals, Midland, MI) and polyoxypropylene diamine (D400; Jeffamine D400 from Huntsman) were mixed in a stoichiometric ratio (amino hydrogen : epoxide functions = 1). The nematic LC mixture (BL001, also designated E7; Merck, Darmstadt, Germany) was added at a concentration of 50 wt % to provide an isotropic liquid homogeneous solution at 20°C (see Fig. 1 for the chem-

ical structures of these materials). Mixing at room temperature required about 10 min and the solution was kept for at least 1 h without significant polymerization or phase separation. At this temperature, the extent of reaction was negligible (<3%) for several hours.

Electrooptical cells were prepared as follows: the homogeneous solution was sandwiched between two ITO-coated glass plates (Balzers, Liechtenstein); the PDLC was formed by thermal polymerization of the epoxy-amine precursors, in an oven, with a temperature cure cycle that will be detailed later.

Samples exhibiting thicknesses between 5 and 40 μm were obtained using appropriate spacers. The film thickness was measured after the formation process of the PDLC film by a micrometer caliper (uncertainty: $\pm 1 \mu\text{m}$; Mitutoyo, Japan). For each reaction conversion, a large number of samples were prepared to check for reproducibility, especially that of the electrooptical curve.

Differential scanning calorimetry (DSC)

DSC was performed on the same samples that were used for electrooptical characterization [i.e., samples that were cured under exactly the same conditions (in ITO-coated glass cells)]. Scans were carried out from -100 to 320°C at $10^\circ\text{C}/\text{min}$ to determine, on the first heating run, the two glass-transition temperatures (T_g^α and T_g^β of the polymer-rich and LC-rich phases, respectively), the nematic-isotropic (N-I) transition temperature (T_{N-I}) of the LC-rich phase and the residual polymerization enthalpy $[\Delta H_{r(p)}]$, where p is the polymerization conversion (i.e., cure extent or reaction conversion) defined as $p = 1$:

$$\frac{\Delta H_{r(p)}}{\Delta H_0} \quad (1)$$

where ΔH_0 is the total exothermic enthalpy of the epoxy-amine reaction, previously reported in the literature, and $\Delta H_0 = 99 \pm 3 \text{ kJ}$ per epoxy equivalent.^{7,8} T_g values were measured as the temperature midpoint between the tangents of the two baselines above and below the glass-transition region (inflection point). T_{N-I} was taken as the maximum of the endothermic peak.

Scanning electron microscopy (SEM)

SEM observations were made at Centre Technologique des Microstructures-Centre de Microscopies Electroniques Appliquées à la Biologie et la Géologie (CMEABG) of University Lyon 1. An ElectroScan Explorer SEM was used under wet

atmosphere at a pressure of 4.5 Torr. Accelerating voltage was fixed at 25 kV and temperature at 6°C .

The samples used were also those prepared for electrooptical characterization and were fractured in liquid nitrogen. The observation was made *in situ* by either of the following: the fractured surface was washed rapidly (3 min) with methanol so that holes could be observed, or, the LC was not extracted and the sample was observed directly after fracturing the surface where the LC was still present.

The micrographs obtained from the two preparation methods revealed analogous morphologies in terms of mean diameter and diameter distribution. However, on some samples, prepared without methanol washing, the LC was seen to exude out of the fractured surface (see Fig. 3, below, on the micrograph at conversion of 75%), thus hiding the droplets.

Electrooptical measurements

A standard setup was used to measure the transmission properties of PDLC films at room temperature. The PDLC cells were oriented normal to the beam of an unpolarized HeNe laser ($\lambda = 632.8 \text{ nm}$). The transmission values were corrected using appropriate calibration standards.

To evaluate the electrooptical properties of the PDLC films, light transmission changes upon application of an ac electrical field of frequency 145 Hz were investigated. Starting from the off-state, a linear increasing voltage ramp was applied up to a desired maximum value V_{max} , followed by a similar decrease of the voltage. The whole scan up and down ramp took 120 s; an additional measuring time of 60 s followed the relaxation behavior of the transmittance in the off-state. The same procedure was repeated several times using the same sequence of appropriate voltage maximum values.

RESULTS AND DISCUSSION

Cure cycle

The PDLC was formed by polycondensation in a two-step temperature cure (Fig. 2). This cure first applied the polymerization at 100°C in an isotropic medium up to a reaction conversion called p_1 ; then a second step at 30°C until a polymerization conversion, called p_2 , where samples are analyzed. The change from 100 to 30°C was carried out in about 3 min. The glass-transition temperatures of both polymer-rich and LC-rich phases at the conversion p_1 were below 25°C . Therefore the reacting systems did not vitrify so that the polymerization was able to continue and even be completed at 30°C .

The formation process of such PDLCs is a combination of polymerization and thermal induced phase

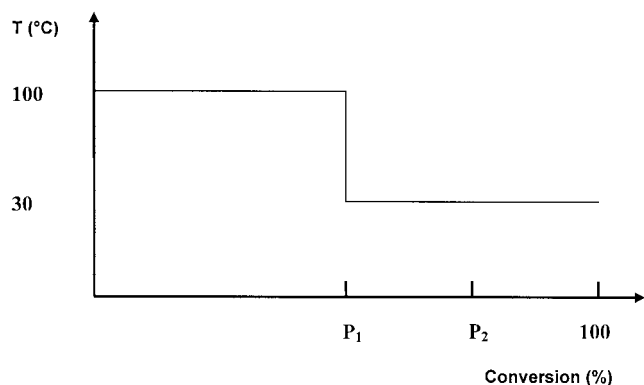


Figure 2 Polymerization cure cycle ($p_1 + p_2$) and conversions (p_2) at which electrooptical and morphology analyses are performed: $p_1 = 59\%$ for all samples; $p_2 = 60, 75, \text{ or } 90\%$.

separation. The advantage of a two-step cure was shown to provide controlled variation of the LC droplet final size according to the conversion p_1 at which the cure temperature changed from 100 to 30°C.^{8,9}

The gel conversion of this system was previously measured at $p_{\text{gel}} \sim 60\%$,^{8,9} which means that the samples under investigation were near or beyond the gel point. Polycondensation of diepoxide/diamine monomers (2 + 4 functionalities) yielded significantly higher gel conversion than crosslinking from free-radical polymerization,⁷ for which $p_{\text{gel}} < 10\%$ and where phase separation of an additive often overlaps with gelation of the matrix. In our case, phase separation can be decorrelated from gelation.

The kinetics of the epoxy-amine reaction in the presence of 50 wt % of LC were previously investigated^{8,9} at each isothermal temperature of 100 or 30°C. Following these lines, we chose to investigate three PDLCs that were all first polymerized at 100°C to reach a monomer conversion of $p_1 \approx 59\%$. In the second step, a postcure at 30°C was performed for either 1, 5, or 30 days leading to epoxy conversions of $p_2 = 60, 75, \text{ and } 90\%$ (see Table I below). All three samples ($p_2 = 60, 75, \text{ or } 90\%$) were phase separated at 30°C to enable an electrooptical analysis at the conversion p_2 . They were thus composed of a dispersed LC-rich phase and a swollen polymer network.

Evolution of morphology of LC droplets at three polymerization conversions

The first parameters likely to affect the electrooptical characteristics are the mean diameter and number density of the nematic droplets. Figure 3 shows the evolution of the micrographs (SEM) at three different polymerization conversions and the corresponding image analyses.

A random distribution of holes with nearly spherical shape (i.e., the former droplets) was observed for

the three conversions. A slight increase in their number-average diameter (and also a broadening of the size distribution) with the cure extent was calculated (Fig. 3). Furthermore, some coalescence is present because the calculated number density of droplets tends to decrease with conversion: 8.5 then 7 then 6.5 nodules/cm² for, respectively, $p = 60, 75, \text{ and } 90\%$. (The seemingly double population of droplet size on the micrograph at $p = 60\%$ is probably attributable to the smaller area analyzed.) These characteristics are consistent with a nucleation-growth mechanism, which may be coupled with a secondary nucleation² that occurs isothermally at 30°C and provides a morphology superimposed on that present on cooling.

Phase separation was never experimentally detected in the isotropic phase at 100°C, although theoretical considerations predicted an isotropic liquid-liquid phase separation at this temperature.^{10,11} However, even if initial phase separation may have been an isotropic liquid-liquid demixing at 100°C, the nematic phase appears only when cooling from 100 to 30°C. Therefore the nematic droplets are able to grow isothermally at 30°C (between p_1 and p_2) during the postcure time allowed before electrooptical measurement.

In conclusion the variation of the mean diameter and droplet number density is small and is not able to explain the dramatic change in transmittance-voltage curves, as discussed below.

Properties of the sol and gel fractions

In the postgel stage, the polymer is composed of one molecule (gel fraction) and a distribution of reactive i-mers, not yet chemically linked to the gel (sol fraction).

Characteristics of sol fraction (sol)

To determine the mass-average molar mass of the sol fraction we used statistical models of polycondensation in the postgel stage.¹⁰⁻¹³

The mass fraction of sol W_s is expressed by

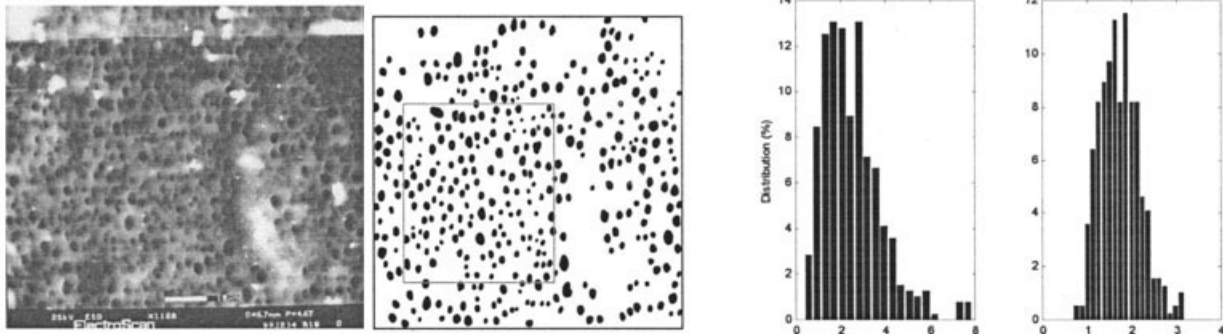
$$W_s = W_{\text{DA}}x^4 + W_{\text{DGEBA}}(px^3 + 1 - p)^2 \quad (2)$$

$$x = [(1/p^2) - 0.75]^{1/2} - 0.5 \quad (3)$$

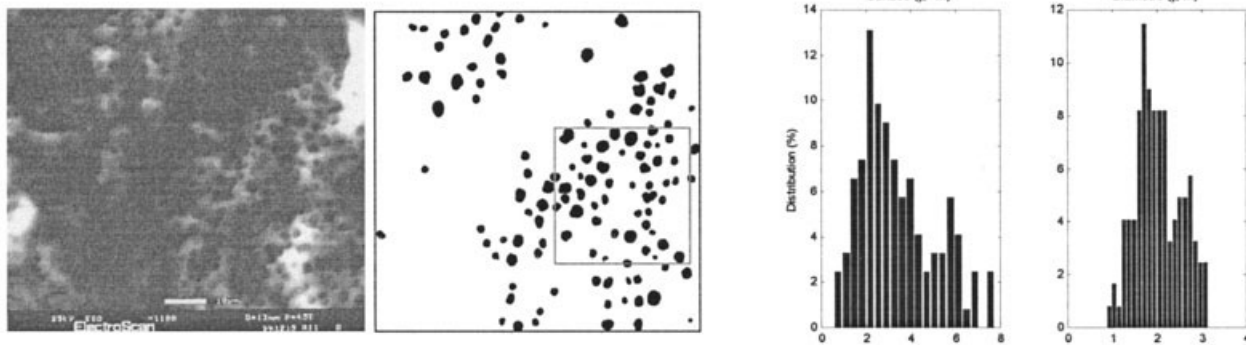
where W_{DA} and W_{DGEBA} are, respectively, the mass fractions of the diamine and diepoxide monomers ($W_{\text{DA}} + W_{\text{DGEBA}} = 1$); p is the overall polymerization conversion, here obtained by DSC [eq. (1)]; and x is the probability of seeing a finite chain when looking out from a randomly chosen amino hydrogen.^{7,10,11}

The conversion of amino-hydrogen functions in the sol fraction is given by

$p = 60\%$



$p = 75\%$



$p = 90\%$

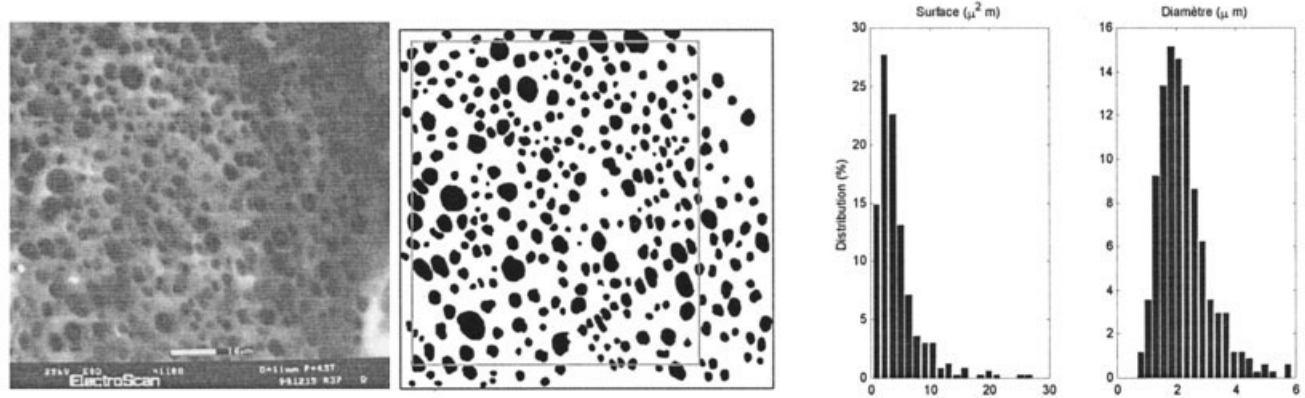


Figure 3 SEM micrographs at conversions of $p = 60, 75,$ or 90% .

TABLE I
Transition Temperatures of LC-Rich and Polymer-Rich Phases (DSC Values), Calculated Characteristics of the Sol Fraction (Mass-Average Molar Mass of the Sol Fraction \bar{M}_w^{sol} , Weight Fraction of Sol W_s), and Gel Fraction (Concentration of Elastic Chains per Unit Volume of Gel ν_e , Weight Fraction of Gel W_g) at Conversions of $p = 60, 75, \text{ and } 90\%^a$

p^a (%)	T_{N-1} (°C)	$T_{g \times \text{exp}}^\alpha$ ^b (°C)	$T_{g \times \text{exp}}^\beta$ ^b (°C)	\bar{M}_w^{sol} (g/mol)	ν_e (mol/unit volume of gel)	W_g (weight fraction)
60	43	-15	-60	27900	1×10^{-6}	0.15
75	56	-6	-60	1500	2×10^{-4}	0.90
90	60	0	-62	440	6.3×10^{-4}	0.99
100	60	5	-62	—	6.5×10^{-4}	1

^a p , conversion at which calorimetric and electrooptical analysis were performed.

^b α refers to the polymer-rich phase; β refers to the LC-rich phase. $T_{g \times \text{exp}}^\alpha$ or $T_{g \times \text{exp}}^\beta$ glass-transition temperatures read on the DSC, first heating runs, at midpoint.

$$p_A = \frac{p}{x}(px^3 + 1 - p) \quad (4)$$

Then the stoichiometric ratio of amino hydrogens to epoxy groups in the sol is given by

$$r_{\text{sol}} = \frac{x^4}{(px^3 + 1 - p)^2} \quad (5)$$

Finally, the mass-average molar mass of the sol fraction is expressed by

$$\bar{M}_w = \frac{r_{\text{sol}}/2[1 + r_{\text{sol}}p_A^2]M_{\text{DA}}^2 + [1 + 3r_{\text{sol}}p_A^2]M_{\text{DGEBA}}^2 + 4r_{\text{sol}}p_A M_{\text{DA}}M_{\text{DGEBA}}}{[r_{\text{sol}}/2M_{\text{DA}} + M_{\text{DGEBA}}][1 - 3r_{\text{sol}}p_A^2]} \quad (6)$$

where M_{DA} is the molar mass of the diamine monomer and M_{DGEBA} is the molar mass of the diepoxy monomer.

Table I shows the calculation of the mass average molar mass of the epoxy-amine i-mers of the sol fraction at the three conversions chosen.

Characteristics of gel fraction (gel)

One main characteristic of the gel fraction is the concentration of crosslinking points per unit volume of gel, given by

$$[X_3] = \frac{2(1-x)^4 + 4x(1-x)^3}{W_g(V_{\text{DA}} + 2V_{\text{DGEBA}})} \quad (7)$$

where V_{DA} and V_{DGEBA} are, respectively, the molar volume of diamine and diepoxy monomers ($V_{\text{DA}} = 364 \text{ cm}^3 \text{ mol}^{-1}$; $V_{\text{DGEBA}} = 298 \text{ cm}^3 \text{ mol}^{-1}$). W_g is the gel fraction ($W_g = 1 - W_s$).

In the particular case of the monomers used, the diamine is considered long and flexible compared to the diepoxide structure; therefore the DA is consid-

ered elastically active, whereas the DGEBA is considered rigid.^{14,15} The crosslinks are considered to have a functionality of 3.^{10,12}

The concentration of elastic chains per unit volume of gel is given by

$$\nu_e = \frac{1}{2}[X_3] \quad (8)$$

From eqs. (1)–(8), \bar{M}_w , W_g , and ν_e were calculated at $p = 0.60$ (60%), 0.75 (75%), and 0.90 (90%) and the values obtained are reported in Table I.

Evolution with conversion of parameters characterizing the sol and gel polymer fractions and correlation to the electrooptical behavior

Sol fraction

The i-mers not chemically linked to the network are the only polymeric molecules that are likely to be soluble in the nematic phase. Furthermore, it was calculated that the nematic phase exhibits an exclusion effect toward the high molar mass molecules of the sol-fraction distribution; that is, the nematic phase accepts only monomers, dimers, and trimers in the case of the thermosetting matrix considered (DGEBA-D400).¹¹

At a conversion of 90%, the sol fraction contains molecules whose mass-average molar mass has decreased to $\bar{M}_w^{\text{sol}} = 440 \text{ g mol}^{-1}$ (i.e., almost exclusively monomers) (Table I) but this sol fraction represents only 1 wt % of the polymer molecules ($W_s = 0.01$). Thus the presence of residual monomers in the LC-rich phase is fairly weak, and the electrooptical properties will depend only weakly on the characteristics of the sol fraction (weight fraction of uncrosslinked i-mers, molar mass of i-mers).

On the contrary, at a conversion of 60%, the sol fraction represents 85 wt % of the polymer molecules ($W_s \approx 0.85$) (Table I) and contains molecules of mass-average molar mass $\bar{M}_w^{\text{sol}} = 27,900 \text{ g mol}^{-1}$ (showing a

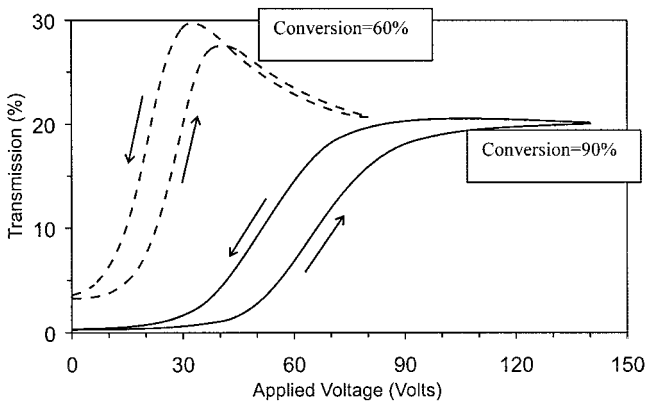


Figure 4 Electrooptical curve (transmission–voltage curve) of 30- μm -thick PDLC at conversions of $p = 60$ and 90%.

large distribution). Thus, the much greater occurrence of soluble monomers or oligomers (dimers or trimers) in the nematic phase will act as pollutants. Consequently, T_{N-I} of the LC-rich phase is significantly lower than that of neat LC.

One consequence for the electrooptical curve (Fig. 4) is that transmission in both the off-state (T_{off}) and on-state (T_{on}) decreases with the extent of cure (see also Figs. 5 and 6). Given that the droplet size and the droplet number density do not change drastically above the gel point, T_{off} and T_{on} are mainly affected by a change of the refractive indices of the nematic phase and the sol fraction.

Interestingly, in Figures 5 and 6 (representing T_{off} and T_{on} in a logarithmic scale as a function of the PDLC thickness), the off-state transmission decreases linearly with a change of slope at a given thickness and the decrease in the off-state is more rapid for the conversion at 90%. These results indicate that the scattering cross section evolves during the course of the reaction. Again there should be a significant variation of both ordinary and extraordinary LC and polymer

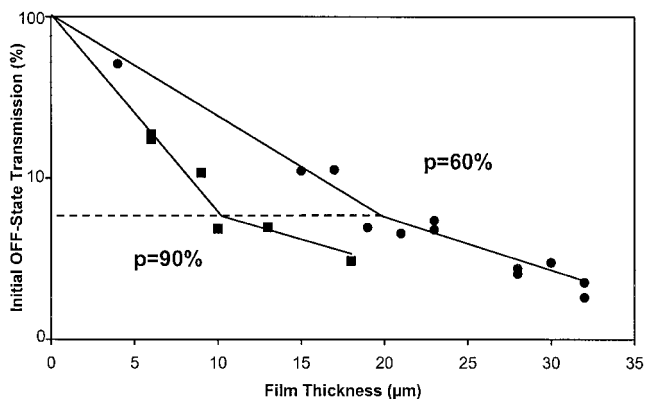


Figure 5 Off-state transmission (T_{off}) versus film thickness at conversions of $p = 60$ and 90%.

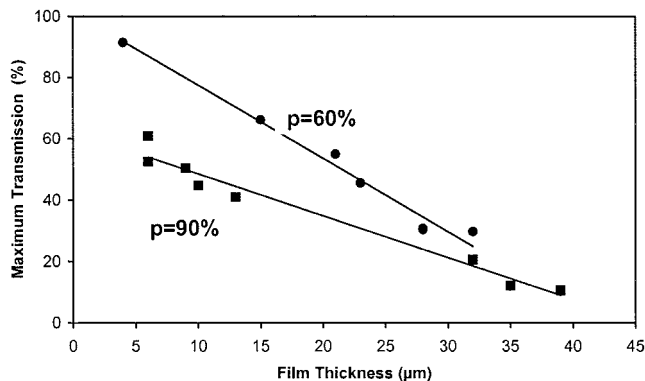


Figure 6 Maximum on-state transmission (T_{on}) versus film thickness at conversions of $p = 60$ and 90%.

refractive index. The T_{on} variation (Fig. 6) calls for similar remarks.

Figure 7 illustrates the dependency of threshold voltage (V_{10}) on film thickness. Striking differences can be found between the two conversions: 60% shows much lower V_{10} values than those at 90% and increasing the film thickness leads to a nonlinear behavior at 60%, whereas the 90% conversion shows the expected linear dependency.

To explain the increase in threshold voltages with the reaction conversion, one must consider the role of solubility of i-mers in the LC-rich phase, at conversions near the gel point, and also that of a still loose network matrix ($W_g = 0.15$, $\nu_e = 10^{-6}$ mol/unit volume of gel at $p = 60\%$) (Table I). When the network is easily swollen, one expects a loose interface between the LC-rich and polymer-rich phases giving rise to lower switching voltages [compared to a nearly pure LC phase at conversions well above the gel point (e.g., 90%), showing a sharp interface with little or no swelling].

Gel fraction

The network elasticity (reflected by ν_e) changes dramatically with conversion: the concentration of elastic

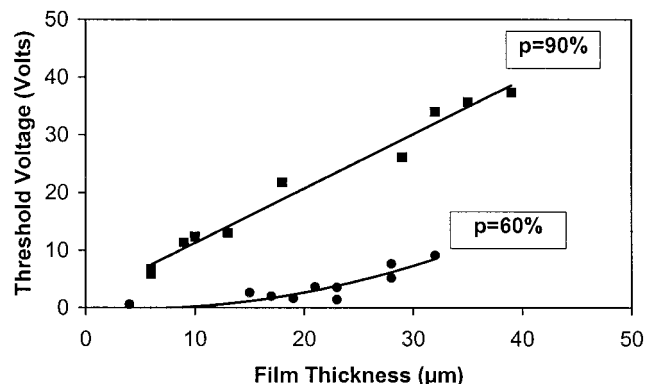


Figure 7 Threshold voltage at 10% transmission (V_{10}) versus film thickness at conversions of $p = 60$ and 90% (first voltage cycle, ramp up, $\lambda = 632.8$ nm, $\nu = 145$ Hz).

chains is increased by more than two orders of magnitude from near the gel point at $p = 60\%$, where $\nu_e = 10^{-6}$ mol/unit volume of gel, to $p = 75\%$ ($\nu_e = 2 \times 10^{-4}$), and further to $p = 90\%$ ($\nu_e = 6.3 \times 10^{-4}$). Meanwhile the gel fraction (W_g) changes from 0.15 to 0.99 (Table I). In such a change, the polymer gel progresses from a very loose network to a network that has attained the order of magnitude of the fully crosslinked network (ν_e at $p = 90\%$ is nearly equal to $\nu_e^\infty \approx 6.5 \times 10^{-4}$ mol/unit volume of gel).

As a result, the electrooptical curve exhibits behavior attributed to the change of elastic properties. On the transmission–voltage curve at 60% conversion (Fig. 4), the maximum transmission is reached for a voltage lower than the maximum applied voltage. Further increasing the electric field leads to a decrease in the transmission of the sample and a constant value characterizing the on-state was not observed.

We assume that at conversion $p \approx 60\%$, the nascent network is deformed at high fields by the orientation of the LC droplets. The network deformation is accompanied by an increase in the number of scattering centers and consequently the T_{on} transmittance decreases at high voltage (>30 V, Fig. 4). In contrast, the electrooptical curves at higher conversions (e.g., 75%) exhibit a “classical” behavior because the crosslink density is fixed and is sufficiently high for the polymer network not to be deformed.

CONCLUSIONS

PDLCs (blends of diepoxy–diamine thermosetting polymer and E7 nematic liquid crystal 50 wt %) were processed by two-step thermal cures (a high-temperature cure followed by a postcure at low temperature), resulting from a combination of polymerization and thermally induced phase separation. We investigated the electrooptical behavior of a PDLC at three polymerization conversions after the gel point. In this conversion range, the droplets have a relatively constant mean diameter between 1.7 and 2.2 μm , which enables

the study of the role of other parameters such as sol and gel polymer fractions.

The transmission versus voltage curves were closely reproducible for each reaction conversion considered but showed remarkable changes with the cure extent (i.e., the polymerization conversion), especially near the gel conversion. The evolution in either the LC-phase composition (presence of uncrosslinked oligomers from the sol fraction) or in the elastic properties of the network matrix (elastic chain density of the gel fraction) is responsible for modifications of off- and on-state transmissions, threshold, and saturation voltages.

This study highlights the importance of ensuring controlled cure cycles in thermoset-based PDLCs to produce stable materials.

References

1. Williams, R. J. J.; Rozenberg, B. A.; Pascault, J.-P. *Adv Polym Sci* 1997, 128, 95.
2. Paul, D. R.; Bucknall, C. B., Eds. *Polymer Blends*; Wiley-Interscience: New York, 1999; Vol. 1, pp. 379–415.
3. Crawford, G. P.; Zumer, S. *Liquid Crystals in Complex Geometries*; Taylor & Francis: London, 1996.
4. Higgins, D. A. *Adv Mater* 2000, 12, 251.
5. Maschke, U.; Coqueret, X.; Benmouna, M. *Macromol Rapid Commun* 2002, 23, 159.
6. Eston, S.; Sambles, R., Eds. *The Optics of Thermotropic Liquid Crystals*; Taylor & Francis: London, 1998; Chapter 11.
7. Pascault, J.-P.; Sautereau, H.; Verdu, J.; Williams, R. J. J., Eds. *Thermosetting Polymers*; Marcel Dekker: New York, 2002.
8. Masood Siddiqi, H.; Dumon, M.; Eloundou, J. P.; Pascault, J.-P. *Polymer* 1996, 37, 4795.
9. Masood Siddiqi, H.; Dumon, M.; Pascault, J.-P. *Mol Cryst Liq Cryst Sci Technol* 1998, 312, 137.
10. Borrajo, J.; Riccardi, C. C.; Williams, R. J. J.; Masood Siddiqi, H.; Dumon, M.; Pascault, J.-P. *Polymer* 1998, 39, 845.
11. Riccardi, C. C.; Williams, R. J. J.; Masood Siddiqi, H.; Dumon, M.; Pascault, J.-P. *Macromolecules* 1998, 31, 1124.
12. Miller, D. R.; Macosko, C. W. *Macromolecules* 1976, 9, 206.
13. Miller, D. R.; Macosko, C. W.; Valles, E. M. *Polym Eng Sci* 1979, 19, 272.
14. Dusek, K.; Ilavsky, M.; Somvasky, J. *Polym Bull* 1987, 18, 209.
15. Williams, R. J. J.; Riccardi, C. C.; Dusek, K. *Polym Bull* 1991, 25, 231.